Ribosomal S6 kinase 2 interacts with and phosphorylates PDZ domain-containing proteins and regulates AMPA receptor transmission

Gareth M. Thomas, Gavin R. Rumbaugh, Dana B. Harrar*, and Richard L. Huganir†

Department of Neuroscience and Howard Hughes Medical Institute, The Johns Hopkins University School of Medicine, 725 North Wolfe Street, Baltimore, MD 21205

Contributed by Richard L. Huganir, September 6, 2005

Extracellular signal-regulated kinase (ERK) signaling is important for neuronal synaptic plasticity. We report here that the protein kinase ribosomal S6 kinase (RSK)2, a downstream target of ERK, uses a C-terminal motif to bind several PDZ domain proteins in heterologous systems and *in vivo*. Different RSK isoforms display distinct specificities in their interactions with PDZ domain proteins. Mutation of the RSK2 PDZ ligand does not inhibit RSK2 activation in intact cells or phosphorylation of peptide substrates by RSK2 *in vitro* but greatly reduces RSK2 phosphorylation of PDZ domain proteins of the Shank family in heterologous cells. In primary neurons, NMDA receptor (NMDA-R) activation leads to ERK and RSK2 activation and RSK-dependent phosphorylation of transfected Shank3. RSK2–PDZ domain interactions are functionally important for synaptic transmission because neurons expressing kinase-dead RSK2 display a dramatic reduction in frequency of AMPA-type glutamate receptor-mediated miniature excitatory postsynaptic currents, an effect dependent on the PDZ ligand. These results suggest that binding of RSK2 to PDZ domain proteins and phosphorylation of these proteins or their binding partners regulates excitatory synaptic transmission.

extracellular signal-regulated kinase | glutamate receptors | RAS | synaptic plasticity

Several forms of synaptic plasticity, including hippocampal long-term potentiation (a cellular model of learning and memory) require signaling through extracellular signal-regulated kinase (ERK) (1–4). ERK signaling also regulates two cellular processes closely associated with plasticity: synaptic delivery of AMPA-type glutamate receptors (AMPA-Rs) (3), and activity-dependent dendritic spine modifications (5, 6).

ERK phosphorylates and activates the p90 ribosomal S6 kinase (RSK) family of protein kinases *in vitro* (7, 8) and *in vivo* (9, 10). Of the four mammalian RSK isoforms, RSK1–RSK4 (11–13), RSK2 and RSK3 are prominent in brain regions, such as cortex and hippocampus, which are important for learning and memory (14). In humans, *RSK2* gene mutations cause Coffin–Lowry syndrome, a condition characterized by psychomotor retardation (15), whereas *RSK2* knockout mice perform poorly in a watermaze spatial learning task and display poor coordination (16). These findings suggest that RSK2 is required for correct neuronal development and/or function and that other RSKs cannot compensate for the loss of RSK2.

Interactions with specific binding partners target many protein kinases to precise cellular locations. In neurons, kinase targeting of this type may control phosphorylation-dependent synapse-specific modifications that in turn underlie many forms of synaptic plasticity (17, 18). Scaffold proteins for elements of the ERK cascade have been described (19, 20), but it is unclear whether and how ERK signaling is targeted to subcellular regions, such as synapses in neurons.

Here we report that RSKs contain C-terminal sequences that bind PDZ [postsynaptic density fraction (PSD)95/discs large/ZO-1] domains, protein–protein interaction domains found in many synaptic proteins (21, 22). RSK2 binds several PDZ domain proteins *in vitro* and *in vivo*. The RSK2 C-terminal PDZ ligand is essential not only for binding to these interactors but also for RSK2 to efficiently phosphorylate them. Furthermore, interactions with PDZ domain proteins are important for RSK2's effects on synaptic function because kinase-dead RSK2 dramatically affects frequency of AMPA-R-mediated miniature excitatory postsynaptic currents (mEPSC) in a PDZ ligand-dependent manner.

Materials and Methods

Antibodies. The following antibodies were used: anti-Shank1 (Chemicon), anti-pan-Shank (M. Sheng, Massachusetts Institute of Technology, Cambridge), anti-Shank3 (P. Worley and J.-C. Tu, The Johns Hopkins University), anti-membrane-associated guanylate kinase with inverted orientation (anti-MAGI-1; Sigma), anti-hemagglutinin (anti-HA) (Roche Applied Science); anti-myc (Covance, Richmond, CA); anti-phospho-RxRxxS/T-(P), anti-phosphoERK, anti-panERK, anti-phosphoRSK S380 (Cell Signaling Technology, Beverly, MA); sheep anti-RSK2 (P. Cohen, University of Dundee, Scotland). Antiserum against residues 712–734 of murine RSK2 (the same peptide used to generate sheep anti-RSK2 antibody) was raised in rabbits and affinity-purified. Anti-glutamate receptor-interacting protein-1 (anti-GRIP1) antibody is described in ref. 23.

cDNA Clones and Molecular Biology. The noncatalytic C termini of murine RSK2, murine RSK1, and rat RSK3 were subcloned into the pPC97 vector. Truncated (ΔC) mutants of these constructs lacking the four C-terminal amino acids were generated by PCR. Point mutants were generated with a QuikChange mutagenesis kit (Stratagene). Full-length murine RSK2, with and without its four C-terminal amino acids, was subcloned into mammalian expression vectors. GRIP1 constructs are described in ref. 23. The fidelity of all constructs was verified by DNA sequencing.

Yeast Two-Hybrid Screening. The RSK2 C terminus "bait" was used to screen a rat hippocampal cDNA library. Clones that grew

Conflict of interest statement: Under a licensing agreement between Upstate Group, Inc. and The Johns Hopkins University, R.L.H. is entitled to a share of royalty received by the University on sales of products described in this article. R.L.H. is a paid consultant to Upstate Group, Inc. The terms of this arrangement are being managed by The Johns Hopkins University in accordance with its conflict of interest policies.

Abbreviations: ERK, extracellular signal-regulated kinase; RSK, ribosomal S6 kinase; AMPA-R, AMPA-type glutamate receptors; APV, 2-amino-5-phosphonovaleric acid; mEPSC, miniature excitatory postsynaptic current; MEK, mitogen-activated protein kinase kinase; PMA, phorbol 12-myristate 13-acetate; aCSF, artificial cerebrospinal fluid; MAGI, membrane-associated guanylate kinase with inverted orientation; GRIP, glutamate receptor-interacting protein-1; NMDA-R, NMDA receptor; HA, hemagglutinin; PSD, postsynaptic density; wt, wild type.

*Present address: Division of Neuroscience, Children's Hospital, and Program in Neuroscience, Harvard Medical School, Boston, MA 02115.

†To whom correspondence should be addressed. E-mail: rhuganir@jhmi.edu.

www.pnas.org/cgi/doi/10.1073/pnas.0507476102

on quadruple-deficient plates (Leu-, Trp-, His-, Ade-) were selected, and their plasmids were isolated and sequenced. Clones were back-transformed with bait vectors encoding wild type (wt) or the modified C termini of RSK1–RSK3.

HEK293T Cell Transfection. Two-hybrid "hits" were subcloned into a myc-tagged pRK5 vector. For coimmunoprecipitation studies, a calcium phosphate method was used to cotransfect these constructs with full-length HA-RSK2 cDNA into HEK293T cells. Cells were lysed in immunoprecipitation buffer (IPB; PBS, pH 7.4/1 mM EDTA/1 mM EGTA/1 mM sodium orthovanadate/5 mM sodium pyrophosphate/50 mM sodium fluoride/1 mM benzamidine/1 μM microcystin-LR/5 μg/ml leupeptin/0.1% β-mercaptoethanol/1% Triton X-100). After centrifugation, soluble supernatants were immunoprecipitated with anti-myc antibodies precoupled to protein G-Sepharose. Beads were washed once with IPB, twice with IPB plus 0.5M NaCl, and once with IPB. Proteins were eluted with SDS sample buffer, subjected to SDS/PAGE, and immunoblotted with anti-myc or anti-HA antibodies. These and all subsequent biochemical experiments were performed at least three times, and representative experiments are shown.

Immunoprecipitation from Rat Brain. Rat brain P2 fraction was prepared as described in ref. 24, except that the P2 pellet was solubilized at 4°C in binding buffer [50 mM Tris·HCl, pH 7.4/0.1 mM EGTA/0.1% Triton X-100/1 μM microcystin-LR plus Complete protease inhibitors (Roche)]. After centrifugation for 10 min at 100 000 $\times$ *g* at 4°C, soluble supernatant was added to protein G-Sepharose beads precoupled to anti-RSK2 antibody or purified sheep IgG. After incubation for 90 min at 4°C, beads were washed twice with binding buffer before resuspension in SDS sample buffer, SDS/PAGE, and immunoblotting.

Shank1a Phosphorylation by RSK2 in Intact Cells Detected by Phospho-Substrate Antibodies. HEK293T cells transfected with myc-Shank1a plus HA-RSK2wt or HA-RSK2ΔC cDNAs were serum-starved for a further 12 h. U0126 mitogen-activated protein kinase kinase (MEK) inhibitor (10 μM final concentration) or 0.1% DMSO vehicle was then added to the medium for 1 h before cells were stimulated with phorbol 12-myristate 13-acetate (PMA) or left unstimulated in the continued presence of U0126 or DMSO. Cells were lysed as above, and myc-Shank1a was immunoprecipitated. Immunoprecipitates were washed extensively and denatured in SDS sample buffer before SDS/PAGE and immunoblotting with anti-RxRxxS/T(P) antibodies (25).

Activation of ERK and RSK Signaling in Primary Cortical Neurons. Primary cortical neurons (26) used after 15–22 days *in vitro* were transferred to magnesium-free artificial cerebrospinal fluid (aCSF) containing 10 mM Hepes (pH 7.4), 150 mM NaCl, 3 mM KCl, 2 mM $CaCl_2$, 10 mM glucose plus 200 μM D,L-2-amino-5-phosphonovaleric acid (D,L-APV) and placed at 37°C for 1 h. Cells were washed into aCSF either with or without D,L-APV, or stimulated with PMA and then placed at 37°C for 30 min. U0126 (10 μM) or DMSO vehicle was added to the initial aCSF and all washes. Neurons were lysed with neuronal lysis buffer (25 mM Tris·HCl, pH 7.5/0.25 M NaCl/5 mM EDTA/5 mM EGTA/50 mM sodium fluoride/1 mM sodium orthovanadate/2% Triton X-100/1 μM microcystin-LR plus Complete protease inhibitors). Cell suspension was centrifuged, and the supernatants were used for subsequent experiments.

Transfection of Cortical Neurons. Neurons (as above) were incubated at 37°C in Hepes-buffered DMEM containing APV and transfected with myc-Shank3 or empty vector DNA (6 μg per dish) using a Lipofectamine-based method. After transfection (1 h) and recovery in culture medium (24 h), cells were washed into aCSF plus APV with U0126 or DMSO vehicle and stimulated as above. After stimulation, cells were lysed and myc immunoprecipitates were prepared and processed, as for Shank1 phosphorylation in HEK293T cells, before detection with RxRxxS/T(P) antibody.

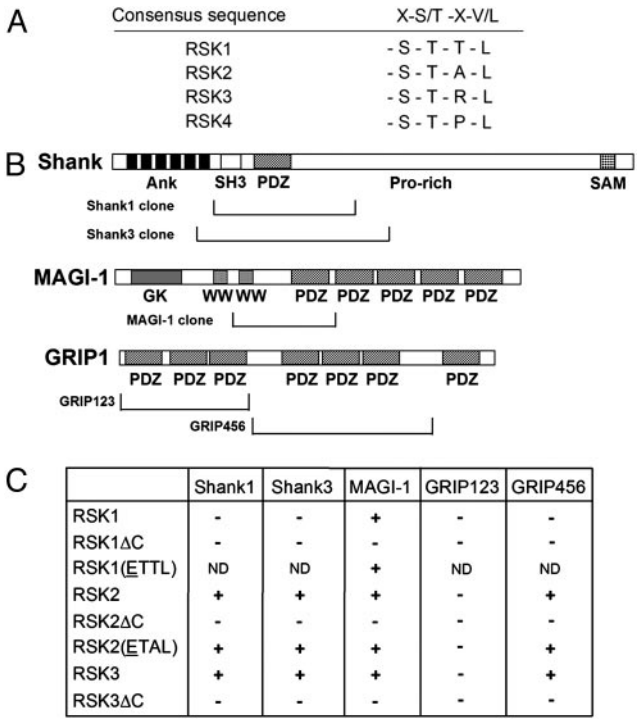

C

	Shank1	Shank3	MAGI-1	GRIP123	GRIP456
RSK1	-	-	+	-	-
RSK1ΔC	-	-	-	-	-
RSK1(ETTL)	ND	ND	+	ND	ND
RSK2	+	+	+	-	+
RSK2ΔC	-	-	-	-	-
RSK2(ETAL)	+	+	+	-	+
RSK3	+	+	+	-	+
RSK3ΔC	-	-	-	-	-

Fig. 1. RSK2 binds PDZ domain proteins in the yeast two-hybrid system. (*A*) C termini of the four mammalian RSK isoforms are aligned below a Type I PDZ ligand consensus. (*B*) Shank and MAGI-1 cDNA clones isolated from a yeast two-hybrid screen using RSK2 as bait are aligned below a schematic of full-length Shank and MAGI-1 proteins, together with previously described GRIP1 cDNAs (23): Ank, Ankyrin repeats (seven present in Shank1a and five present in Shank3); SH3, Src homology 3 domain; SAM, sterile α-motif; GK, guanylate kinase domain. (*C*) Specificity of the interaction between RSKs and PDZ proteins determined by transformation of yeast with the indicated cDNAs.

Electrophysiology and mEPSC Analysis. Forebrain cultures (15–22 days *in vitro*) in the absence of APV were transfected as above with GFP-tagged RSK2 constructs. Whole-cell patch-clamp recordings were performed 24–36 h later from RSK2-transfected cells or untransfected neighbors. AMPA-R-mediated mEPSCs were isolated as described in ref. 27. Data from each group were averaged, and statistical significance was determined by Student's *t* test. All experiments were performed from at least two individual platings of neurons.

Results

RSKs Bind PDZ Domain Proteins in the Yeast Two-Hybrid System. We hypothesized that a C-terminal sequence (STXL) present in all four mammalian RSK isoforms (Fig. 1*A*) might bind to PDZ domains and thus target RSKs to specific PDZ domain-containing protein complexes. The RSK2 C terminus (residues 681–740) was therefore used as bait in a yeast two-hybrid screen of a rat hippocampal cDNA library. Several positive clones containing PDZ domains were isolated. These clones included Shank1 (Src homology 3 domain and Ankyrin repeat-containing protein-1), and the closely related Shank3 [also known as ProSAP2 (proline-rich synapse associated protein-2)] (28).

BIOCHEMISTRY

Shanks/ProSAPs link NMDA receptor (NMDA-R)-signaling complexes with metabotropic glutamate receptors and the cytoskeleton (29–31). The Shank clones interacting with RSK2 encompassed central regions of Shank1 (amino acids 368–932) and Shank3 (amino acids 358–986), which contained a PDZ domain (Fig. 1*B*).

Another cDNA clone capable of binding to RSK2 encoded a rat ortholog of MAGI-1 (32). The MAGI-1 cDNA clone encompassed a short region [amino acids 325–577 of murine MAGI-1-$\alpha\beta2\gamma$ (GenBank accession no. AAS77818)] containing a WW domain and the first PDZ domain (Fig. 1*B*).

We also tested the interaction of RSK2 with regions of the PDZ domain containing GRIP1 (23). RSK2 interacted with a construct coding for PDZ domains 4–6 of GRIP1 (GRIP456) (Fig. 1*D*), but not a construct coding for the first three PDZ domains of GRIP1 (GRIP123).

We then back-transformed these hits against the C termini of RSK1 and RSK3. There was a degree of specificity in the interactions of different RSKs with different PDZ domain proteins. Thus, RSK1 did not bind to any Shank or GRIP1 clones but did interact with MAGI-1. However, RSK3 bound to both Shank isoforms, MAGI-1, and the GRIP456 construct (Fig. 1*C*).

Because all of the RSK interactors contained PDZ domains, we examined whether these interactions required the PDZ ligand of RSKs. RSK mutants (RSK1ΔC, RSK2ΔC, and RSK3ΔC) lacking the four C-terminal amino acids (thus eliminating the PDZ ligand) did not bind any of the identified PDZ domain proteins, suggesting that the RSK PDZ ligand was responsible for all interactions observed (Fig. 1*C*).

The serine residue in the PDZ ligand (STTL) of RSK1 is phosphorylated *in vivo* (8), and phosphorylation is increased upon RSK1 activation. We investigated whether RSK–PDZ domain interactions persisted if this serine or the analogous serine in RSK2 was mutated to glutamate to mimic this phosphorylation given that phosphorylation of PDZ ligands can alter their binding to PDZ domains (33). Binding of RSK2-ETAL to all PDZ domain proteins examined and of RSK1-ETTL to MAGI-1 was maintained (Fig. 1C). This suggests that both inactive and active RSKs likely bind to PDZ domain proteins, a conclusion supported by data from mammalian cells (Fig. 6, which is published as supporting information on the PNAS web site).

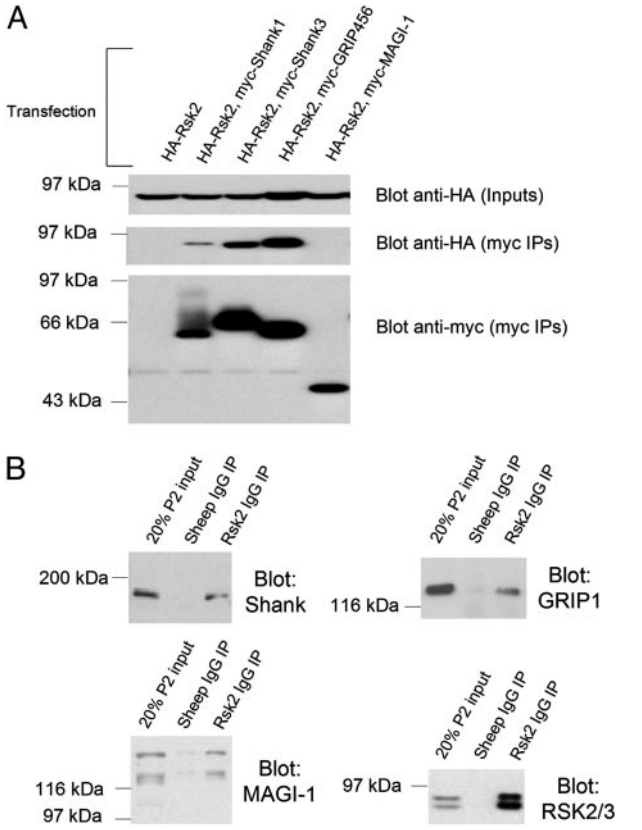

Fig. 2. PDZ domain-containing proteins coimmunoprecipitate with RSK2/3 in heterologous cells and rat brain. (*A*) (*Top* and *Middle*) HEK293T cells were transfected with the indicated constructs, and lysates (*Top*) and myc immunoprecipitates (*Middle*) were immunoblotted with anti-HA antibody. (*Bottom*) Myc immunoprecipitates were blotted with anti-Myc antibody. Molecular mass markers are indicated. (*B*) Immunoblots of Shank (*Upper Left*), MAGI-1 (*Upper Right*), GRIP-1 (*Lower Left*), and RSK2/3 (*Lower Right*) proteins solubilized after extraction of P2 with 0.1% Triton X-100 and present in immunoprecipitates using the indicated antibodies.

RSK2/3 Bind PDZ Domain Proteins in HEK293T Cells and Rat Brain. We next investigated whether RSK–PDZ interactions can occur in mammalian cells. Hits from the two-hybrid screen were subcloned into a myc-tagged vector and coexpressed in HEK293T cells with full-length HA-tagged RSK2. HA-RSK2 was detected in myc immunoprecipitates from HEK293T cells coexpressing HA-RSK2 plus myc-Shank1 (368–932), myc-Shank3 (358–986), or myc-GRIP456 (Fig. 2*A Middle*). However, HA-RSK2 was not detected in myc immunoprecipitates from cells expressing HA-RSK2 alone or from cells coexpressing HA-RSK2 and myc-MAGI-1 (Fig. 2*A Middle*). All myc-tagged proteins were efficiently expressed and immunoprecipitated (Fig. 2*A Bottom*). The failure of the MAGI-1 clone to coimmunoprecipitate HA-RSK2 was surprising because MAGI-1 binds RSK2 in yeast (Fig. 1*C*) and is present in RSK2/3 immunoprecipitates from rat brain (Fig. 3*C*). We speculate that in HEK293T cells the partial MAGI-1 clone may be targeted to a subcellular region that does not contain RSK2.

To investigate whether endogenous RSKs interact with PDZ domain proteins in the brain, we developed a RSK antibody because commercially available RSK2 antibodies display poor sensitivity in brain samples (G.M.T. and R.L.H., unpublished data). Specificity testing with purified RSKs showed that this antibody recognizes RSK2 and RSK3 equally but does not recognize RSK1 (Fig. 7, which is published as supporting information on the PNAS web site). The antibody is henceforth designated a RSK2/3 antibody.

Investigation of RSK2/3 distribution in subcellular fractions from rat brain showed immunoreactivity in soluble fractions (S2), membrane fractions (P2, synaptosomes), and postsynaptic density fractions (PSDI, PSDII, and PSDIII), with two major bands of the predicted molecular masses of RSK2 (83.7 kDa) and RSK3 (83.2 kDa). Only the lower of these bands was present in PSD fractions (Fig. 8, which is published as supporting information on the PNAS web site). This finding suggests that RSK2 and/or RSK3 are present in subcellular fractions (such as P2 and PSDs) that also contain Shank and other PDZ domain proteins, suggesting that RSK2/3 might interact with these proteins *in vivo*.

To investigate this possibility further, we attempted to coimmunoprecipitate PDZ proteins with RSKs from P2 fraction. P2 fraction solubilized with 1% deoxycholate (30) contains several Shank isoforms, but under these conditions no coimmunoprecipitation of PDZ domain proteins with RSK2/3 was detected (data not shown). Because deoxycholate might disrupt RSK–PDZ domain interactions, we performed mild extraction of P2 fraction using 0.1% Triton X-100. The single Shank band solubilized under these conditions coimmunoprecipitated with anti-RSK2/3 antibodies but not purified IgG (Fig. 2*B*). Coimmunoprecipitation was also prevented if RSK2/3 antibodies were preabsorbed with the antigenic peptide (data not shown),

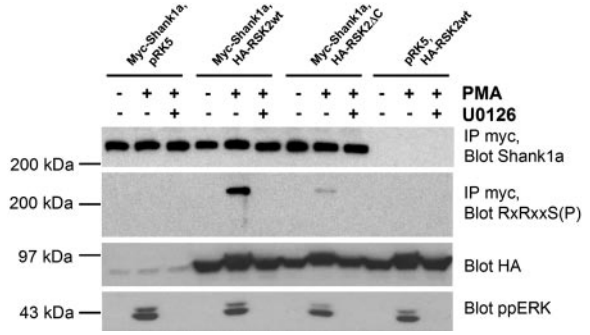

Fig. 3. Phosphorylation of Shank1 at RxRxxS motifs in intact cells requires the RSK2 PDZ ligand. HEK293T cells transfected with full-length myc-Shank1a plus HA-RSK2wt or HA-RSK2ΔC preincubated with U0126 or DMSO vehicle control were then treated with 100 nM PMA for 20 min or left unstimulated. Cells were lysed, and myc immunoprecipitates were blotted for anti-Shank1a or anti-RxRxxS(P). Lysates were blotted for anti-HA or anti-phosphoERK. A cellular cross-reactive band is recognized by anti-HA antibody in the absence of HA-RSK2.

which suggests that RSK2/3 coassociate with Shank proteins in rat brain membrane fractions.

Under similar conditions, we also detected MAGI-1 and GRIP1 in RSK2/3 immunoprecipitates but not in IgG immunoprecipitates. The PDZ domain proteins PSD95 and the sodium/proton exchanger regulatory factor NHERF were absent from RSK2/3 immunoprecipitates (data not shown), suggesting that the interactions described above were specific. None of the above PDZ domain proteins coimmunoprecipitated with RSK1 from P2 fraction (data not shown).

RSK2 Phosphorylates Shank Proteins *in Vitro* and in Intact Cells. Binding of RSKs to PDZ domain proteins might allow specific phosphorylation of these proteins or their binding partners. Shank1 and Shank3 contain several RSK consensus phosphorylation sites (RXRXXS, where X is any amino acid) (34) and both Shanks were efficiently phosphorylated by RSK2 *in vitro* (data not shown). Indeed, RSK2 phosphorylated Shank1 (368–932) with a K_m value (0.17 μM) far below that for the S6 peptide (9.6 μM), a standard RSK2 *in vitro* substrate, suggesting that Shank1 is an extremely good RSK2 substrate (data not shown).

We next investigated whether RSK2 can phosphorylate Shanks in intact cells and whether this phosphorylation requires the RSK2 PDZ ligand. Deletion of the PDZ ligand of RSK2 did not affect the expression level of RSK2 in HEK293T cells, and when cells were treated with PMA to activate ERK/RSK signaling, the kinase activities of HA-RSK2wt and HA-RSK2ΔC constructs assayed against S6 peptide were comparable (Fig. 9, which is published as supporting information on the PNAS web site). This finding suggests that neither RSK2 expression nor activation requires the PDZ ligand.

To investigate phosphorylation of full-length Shank1 by RSK2 in intact cells, we used an antibody that recognizes phosphorylated serine or threonine residues in the motif RxRxxS/T-(P) (25, 35). This antibody specifically recognized Shank1a and Shank3 phosphorylated by RSK2 *in vitro* but not unphosphorylated Shanks or Shanks phosphorylated by ERK2 *in vitro* (Fig. 10, which is published as supporting information on the PNAS web site).

Full-length myc-Shank1 coexpressed in HEK293T cells with HA-RSK2wt was not detectably phosphorylated at RxRxxS/T sites (Fig. 3). However, Shank1 RxRxxS/T phosphorylation increased dramatically after PMA treatment of HA-RSK2-transfected cells (Fig. 3) but was completely prevented by the MEK inhibitor U0126, confirming that a kinase in the ERK

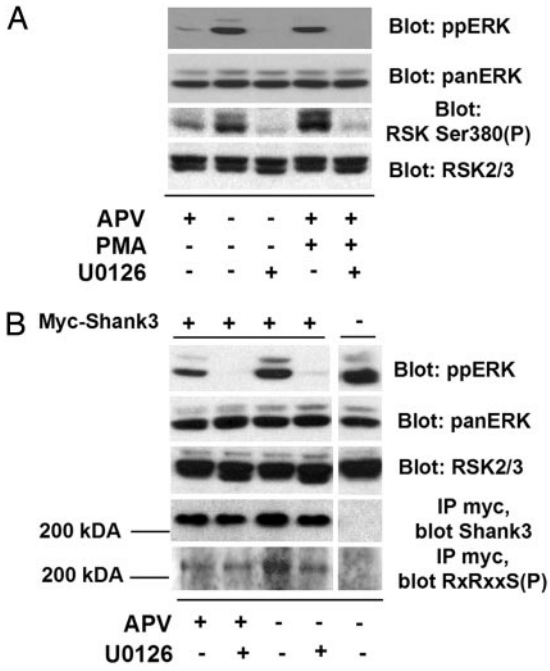

Fig. 4. ERK–RSK signaling triggered by NMDA-R activation leads to phosphorylation of transfected myc-Shank3 in cortical neurons. (*A*) Cortical neurons cultured in D,L-APV were washed into aCSF plus APV in the presence or absence of U0126 and then transferred to aCSF with (+) or without (−) APV or aCSF plus 400 nM PMA for 30 min. Lysates were immunoblotted with the indicated antibodies. (*B*) Cortical neurons transfected with myc-Shank3 cDNA were preincubated in the presence or absence of U0126 and subjected to APV withdrawal (30 min). Lysates were immunoblotted with the indicated antibodies. Myc immunoprecipitates (IP) were immunoblotted with anti-myc antibody (IP myc blot Shank3) and RxRxxS(P) antibody [IP myc, blot RxRxxS(P)].

pathway was responsible for this phosphorylation. RxRxxS/T phosphorylation did not occur in the absence of HA-RSK2 cotransfection, suggesting that HA-RSK2 was the Shank1 RxRxxS/T kinase. In contrast, when Shank1 was cotransfected with HA-RSK2ΔC, PMA-induced RxRxxS/T phosphorylation of Shank1 by HA-RSK2ΔC was far weaker than by HA-RSK2wt (Fig. 3). The reduced phosphorylation of myc-Shank1 by HA-RSK2ΔC was not due to reduced HA-RSK2ΔC expression (Fig. 3, Blot: HA) or decreased ERK activation (Fig. 3, Blot: ppERK). These data suggests that RSK2 phosphorylates myc-Shank1 at RxRxxS/T sites in intact cells and that the RSK2 PDZ ligand is critical for efficient phosphorylation.

We also examined Shank3 phosphorylation by HA-RSK2 *in vitro* and in HEK293T cells by using similar methods. As with Shank1, Shank3 phosphorylation in cells transfected with myc-tagged Shank3 and HA-RSK2 constructs is PMA-dependent, U0126-sensitive, and requires the PDZ ligand of RSK2 (data not shown).

RSK and myc-Shank3 Phosphorylation Are Increased Through ERK Signaling After NMDA-R Activation in Primary Cortical Neurons. We next examined RSK2 activation in cortical neurons by using two stimuli: NMDA-R activation, which is closely linked to synaptic plasticity, and PMA treatment, which potently activates RSK2 in heterologous cells (Fig. 3). In neurons cultured in the presence of the NMDA-R antagonist APV, removal of APV from the culture medium ("APV withdrawal"), triggers NMDA-R activation by endogenous glutamate and rapidly recruits AMPA-Rs to synapses (26). We investigated whether this paradigm also activates ERK/RSK signaling, because ERK activation is required for several forms of synaptic plasticity (1, 3, 4). APV

BIOCHEMISTRY

withdrawal increased phospho-ERK (Fig. 4*A*, Blot: HA) and phospho-RSK levels [Fig. 4*A*, Blot: RSK Ser380(P)]. This activation was rapid (Fig. 11, which is published as supporting information on the PNAS web site). PMA treatment also increased phospho-ERK and phospho-RSK levels. Preincubation of neurons with U0126 before PMA treatment or APV withdrawal reduced phospho-ERK and phospho-RSK signals below control levels without affecting expression of either of these kinases (Fig. 4*A*). Increases in RSK phospho-levels were paralleled by increases in RSK2/3 kinase activity, which was also U0126-sensitive (Fig. 12, which is published as supporting information on the PNAS web site). This finding suggests that RSK activation in cortical neurons occurs via MEK and ERK.

We next examined regulation of Shank phosphorylation by RSKs in cortical neurons. We could not detect phosphorylation of endogenous Shank1 or Shank3 at RxRxxS/T motifs by RSK after APV withdrawal or PMA treatment, perhaps because of a lack of sensitivity of our phospho-antibodies. We could, however, detect phosphorylation of transfected myc-Shank3 at RxRxxS/T sites, which increased after APV withdrawal (Fig. 4*B*). The APV withdrawal-induced increase in Shank3 phosphorylation was sensitive to U0126, implicating a kinase downstream of MEK/ERK that phosphorylates RxRxxS/T motifs. The best candidate for such a kinase is a member of the RSK family.

The PDZ Ligand of RSK2 Is Necessary for Effects on Synaptic Function. RSK2 is required for correct neuronal development and function (15, 16), and kinase-dead mutants of RSK2 function in a dominant-negative fashion, preventing phosphorylation of endogenous RSK2 substrates (36). To investigate whether RSK regulates synaptic transmission, we transfected cortical neurons with a GFP-tagged kinase-dead RSK2 (GFP–RSK2kn) that completely lacks kinase activity *in vitro* (data not shown), and we examined mEPSCs. Transfection of GFP–RSK2kn dramatically reduced the mEPSC frequency of AMPA-R-mediated synaptic transmission compared with untransfected neighboring neurons, with no significant change in mEPSC amplitude (Fig. 5*A*). To investigate whether this effect required the PDZ ligand, neurons were transfected with a kinase-dead RSK2 lacking the PDZ ligand (GFP–RSK2knΔC). This construct had no effect on AMPA-R mEPSC frequency compared with untransfected neighboring neurons (Fig. 5*B*).

These results suggest that GFP-RSK2kn competes with endogenous RSK2, preventing it from phosphorylating PDZ domain proteins or their binding partners, whereas GFP-RSK2knΔC (which cannot bind PDZ domain proteins) cannot mimic this effect. However, GFP-RSK2kn might sterically disrupt PDZ domain protein complexes, and this disruption, rather than the inhibition of RSK2 signaling, might reduce mEPSCs. To distinguish between these possibilities, we transfected cortical neurons with a constitutively active RSK2 (GFP–RSK2 Y707A) (37) in which the PDZ ligand remains intact. We confirmed elevated basal kinase activity of GFP–RSK2YA compared with wt GFP–RSK2 *in vitro* (data not shown). The dramatic reduction in mEPSC frequency seen with GFP–RSK2kn was not observed with GFP–RSK2YA (Fig. 5*C*), indicating that GFP–RSK2kn functions by preventing phosphorylation of PDZ domain proteins by endogenous RSK2, rather than via steric effects on PDZ domain complexes.

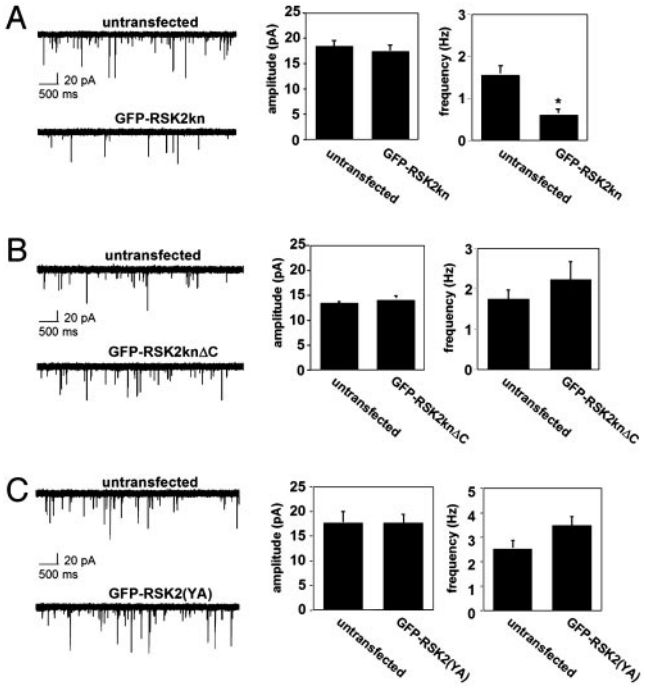

Fig. 5. PDZ ligand-dependent control of AMPA-R transmission by RSK2. (*A*) AMPA-R-mediated mEPSCs isolated from GFP–RSK2kn-transfected cortical neurons or untransfected neighbors. Five overlayed traces per condition (*Left*), mEPSC amplitudes (*Center*), and mEPSC frequencies (*Right*) are plotted. Data are expressed as mean ± SEM: amplitude, 18.33 ± 1.44 pA (untransfected) and 17.32 ± 1.65 pA (GFP–RSK2kn) [$n = 10$ cells (untransfected), $n = 11$ cells (GFP–RSK2kn-transfected), $P > 0.5$]; frequency, 1.54 ± 0.22 Hz (untransfected) and 0.59 ± 0.14 Hz (GFP–RSK2kn) [$n = 11$ cells (untransfected), $n = 10$ cells (GFP–RSK2knΔC-transfected) $P < 0.01$]. (*B*) Neurons were transfected with GFP–RSK2knΔC. Data are expressed as in *A*: amplitude, 16.24 ± 1.25 pA (untransfected) and 15.67 ± 1.31 pA (GFP–RSK2knΔC) ($n = 11$ cells per condition, $P > 0.5$); frequency, 2.23 ± 0.39 Hz (untransfected) and 2.60 ± 0.41 Hz (GFP–RSK2knΔC) ($n = 11$ cells per condition, $P > 0.5$). (*C*) Neurons were transfected with GFP–RSK2 Y707A. Data are expressed as in *A*: amplitude, 17.75 ± 2.35 pA (untransfected) and 17.53 ± 1.78 pA (GFP–RSK2YA) [$n = 12$ cells (untransfected), $n = 14$ cells (GFP–RSK2 YA-transfected), $P > 0.5$]; frequency, 2.51 ± 0.35 Hz (untransfected) and 3.50 ± 0.36 Hz (GFP–RSK2YA) ($n = 12, 14$ cells per condition, $P = 0.06$).

Discussion

The importance of Ras–ERK signaling in neuronal function is increasingly apparent. Here we report an additional level of regulation of ERK signaling through a PDZ domain modulation of the localization and substrate specificity of RSKs. RSKs binding to specific PDZ domain proteins allows phosphorylation of these proteins and may regulate RSK targeting to specific subcellular regions. A previous study reported that RSK2 is associated with a NMDA-R-associated multiprotein complex isolated from forebrain extracts (37). Our results suggest a likely molecular explanation for this finding, because RSK2 directly binds Shank, which is then tethered to NMDA-R protein complexes by Shank interactors, such as guanylate kinase-associated protein (30) or Homer. Despite detecting RSK2/3 in PSDs, however, our immunolabeling studies show that RSK2/3 only weakly colocalizes with synaptic markers in primary hippocampal neurons (G.M.T. and R.L.H., unpublished data). RSK2/3 association with NMDA-R complexes (and Shank itself) may therefore be limited to extrasynaptic or intracellular pools. Consistent with this possibility, the pool of Shank that definitively interacts with RSK2/3 *in vivo* is solubilized by mild detergent (Fig. 2*B*), suggesting that it is not localized within the core PSD.

RSK2/3 interactions with GRIP1 and MAGI-1 *in vivo* also allow potential targeting of Ras–ERK–RSK signaling to phosphorylate these proteins or their binding partners. Like the Shank–RSK2/3 interaction, these complexes are detected in P2 fractions, which are enriched in membrane proteins. Interestingly, mice overexpressing a dominant-negative form of the small G protein Rap1 display reduced membrane-associated ERK

activity and deficits in certain forms of synaptic plasticity and in spatial learning (39). Membrane-associated ERK targets therefore likely play key roles in plasticity and learning. These targets may include membrane-associated RSKs and indirectly the PDZ domain-containing proteins, such as Shank, GRIP1, or MAGI-1, to which RSKs bind.

The dramatic effect of RSK2kn on AMPA-R transmission (Fig. 5) suggests that signaling via RSK2 is important for synaptic transmission. However, the molecular substrate(s) for RSK2 that regulates AMPA-R transmission is unknown. RSK2 efficiently phosphorylates Shank, ablating binding of Shank to cortactin *in vitro* (Fig. 13, which is published as supporting information on the PNAS web site). However, whether this effect modifies synaptic structure and/or transmission is unclear. RSK2-dependent regulation of MAGI-1, GRIP1, or other PDZ domain proteins may instead control AMPA-R transmission.

Although the RSK2kn construct likely functions in a dominant-negative fashion that prevents phosphorylation of PDZ domain proteins by endogenous RSK2, there are several molecular possibilities as to why inhibiting RSK2 might reduce AMPA-R-mediated mEPSC frequency. Reductions in mEPSC frequency classically indicate decreased neurotransmitter release probability from presynaptic terminals (40). However, the percentage of transfected cells in our cultures was low (≈5%); therefore, few presynaptic contacts onto the GFP–RSK2kn-transfected cell from which we recorded contained GFP–RSK2kn. This explanation would therefore imply that the reduced mEPSC frequency is due to a putative retrograde signal that, in turn, affects release probability. Alternatively, expression of the GFP-RSK2kn may alter the number of functional synaptic contacts, perhaps by increasing the percentage of silent synapses (those that contain NMDA-Rs but not AMPA-Rs) or by eliminating synaptic contacts altogether.

Our results may explain why other RSK isoforms cannot compensate for loss of RSK2 in Coffin–Lowry syndrome patients or *RSK2* knockout mice. This lack of compensation is initially surprising, because the kinase domains of different RSK isoforms and their substrate specificities *in vitro* are very similar. However, different RSK isoforms are expressed in strikingly distinct neuronal cell types (14), and the lack of expression of other RSKs in a particular cell type may explain their inability to compensate for RSK2. It is possible that differential expression of RSK isoforms occurs because different RSKs bind and/or phosphorylate distinct PDZ domain proteins in different neuronal cell types. RSK2 targeting to precise protein complexes would allow tight spatial localization of kinase signaling, limiting substrate phosphorylation to precise subcellular regions. It is an intriguing possibility that such signaling localization may underlie neuronal synapse-specific modifications, learning, and memory.

We thank Drs. D. Ginty, P. Worley, J.-C. Tu (all three from The Johns Hopkins University), M. Sheng (Massachusetts Institute of Technology, Cambridge), and R. Erikson (Harvard Medical School, Boston) and Prof. Sir P. Cohen for antibodies and cDNAs. We also thank Dr. J.-C. Beique and other R.L.H. laboratory members and Dr. R. Cole for comments on the manuscript. This work was supported by the Howard Hughes Medical Institute and by National Institutes of Mental Health Grant R01 MH64856-04. G.M.T was supported by a Wellcome Trust International Prize Traveling Fellowship.

1. English, J. D. & Sweatt, J. D. (1997) *J. Biol. Chem.* **272,** 19103–19106.
2. Patterson, S. L., Pittenger, C., Morozov, A., Martin, K. C., Scanlin, H., Drake, C. & Kandel, E. R. (2001) *Neuron* **32,** 123–140.
3. Zhu, J. J., Qin, Y., Zhao, M., Van Aelst, L. & Malinow, R. (2002) *Cell* **110,** 443–455.
4. Thomas, G. M. & Huganir, R. L. (2004) *Nat. Rev. Neurosci.* **5,** 173–183.
5. Wu, G. Y., Deisseroth, K. & Tsien, R. W. (2001). *Nat. Neurosci.* **4**, 151–158.
6. Goldin, M. & Segal, M. (2003) *Eur. J. Neurosci.* **17,** 2529–2539.
7. Sturgill, T. W., Ray, L. B., Erikson, E. & Maller, J. L. (1988) *Nature* **334,** 715–718.
8. Dalby, K. N., Morrice, N., Caudwell, F. B., Avruch, J. & Cohen, P. (1998) *J. Biol. Chem.* **273,** 1496–1505.
9. Erikson, E. & Maller, J. L. (1991) *J. Biol. Chem.* **266,** 5249–5255.
10. Alessi, D. R., Cuenda, A., Cohen, P., Dudley, D. T. & Saltiel, A. R. (1995) *J. Biol. Chem.* **270,** 27489–27494.
11. Alcorta, D. A., Crews, C. M., Sweet, L. J., Bankston, L., Jones, S. W. & Erikson, R. L. (1989) *Mol. Cell. Biol.* **9,** 3850–3859.
12. Zhao, Y., Bjorbaek, C., Weremowicz, S., Morton, C. C. & Moller, D. E. (1995) *Mol. Cell. Biol.* **15,** 4353–4363.
13. Yntema, H. G., van den Helm, B., Kissing, J., van Duijnhoven, G., Poppelaars, F., Chelly, J., Moraine, C., Fryns, J. P., Hamel, B. C., Heilbronner, H., *et al.* (1999) *Genomics* **62,** 332–343.
14. Zeniou, M., Ding, T., Trivier, E. & Hanauer, A. (2002) *Hum. Mol. Genet.* **11,** 2929–2940.
15. Trivier, E., De Cesare, D., Jacquot, S., Pannetier, S., Zackai, E., Young, I., Mandel, J. L., Sassone-Corsi, P. & Hanauer, A. (1996) *Nature* **384,** 567–570.
16. Dufresne, S. D., Bjorbaek, C., El-Haschimi, K., Zhao, Y., Aschenbach, W.G., Moller, D. E. & Goodyear, L. J. (2001) *Mol. Cell. Biol.* **21,** 81–87.
17. Soderling, T. R. & Derkach, V. A. (2000) *Trends Neurosci.* **23,** 75–80.
18. Selcher, J. C., Weeber, E. J., Varga, A. W., Sweatt, J. D. & Swank, M. (2002) *Neuroscientist* **8,** 122–131.
19. Elion, E. A. (2001) *J. Cell Sci.* **114,** 3967–3978.
20. Torii, S., Nakayama, K., Yamamoto, T. & Nishida, E. (2004) *J. Biochem. (Tokyo)* **136,** 557–561.
21. Garner, C. C., Nash, J. & Huganir, R. L. (2000) *Trends Cell Biol.* **10,** 274–280.
22. Kim, E. & Sheng, M. (2004) *Nat. Rev. Neurosci.* **5,** 771–781.
23. Dong, H., O'Brien, R. J., Fung, E. T., Lanahan, A. A., Worley, P. F. & Huganir, R. L. (1997) *Nature* **386,** 279–284.
24. Luo, J., Wang, Y., Yasuda, R. P., Dunah, A. W. & Wolfe, B. B. (1997) *Mol. Pharmacol.* **51,** 79–86.
25. Zhang, H., Zha, X., Tan, Y., Hornbeck, P. V., Mastrangelo, A. J., Alessi, D. R., Polakiewicz, R. D. & Comb, M. J. (2002) *J. Biol. Chem.* **277,** 39379–39387.
26. Liao, D., Scannevin, R. H. & Huganir R. L. (2001) *J. Neurosci.* **21,** 6008–6017.
27. Rumbaugh, G., Sia, G.-M., Garner, C. C. & Huganir, R. L. (2003) *J. Neurosci.* **23,** 4567–4576.
28. Boeckers, T. M., Winter, C., Smalla, K. H., Kreutz, M. R., Bockmann, J., Seidenbecher, C., Garner, C. C. & Gundelfinger, E. D. (1999) *Biochem. Biophys. Res. Commun.* **264,** 247–252.
29. Tu, J. C., Xiao, B., Naisbitt, S., Yuan, J. P., Petralia, R. S., Brakeman, P., Doan, A., Aakalu, V. K., Lanahan, A. A. & Worley, P. F. (1999) *Neuron* **23,** 583–592.
30. Naisbitt, S., Kim, E., Tu, J. C., Xiao, B., Sala, C., Valtschanoff, J., Weinberg, R. J., Worley, P. F. & Sheng, M. (1999) *Neuron* **23,** 569–582.
31. Sheng, M. & Kim, E. (2000) *J. Cell Sci.* **113,** 1851–1856.
32. Dobrosotskaya, I., Guy, R. K. & James, G. L. (1997) *J. Biol. Chem.* **272,** 31589–31597.
33. Chung, H. J., Xia, J., Scannevin, R. H., Zhang, X. & Huganir, R. L. (2000) *J. Neurosci.* **20,** 7258–7267.
34. Leighton, I. A., Dalby, K. N., Caudwell, F. B., Cohen, P. T. & Cohen, P. (1995) *FEBS Lett.* **375,** 289–293.
35. Manning, B. D., Tee, A. R., Logsdon, M. N., Blenis, J. & Cantley, L. C. (2002) *Mol. Cell* **10,** 151–162.
36. Woo, M. S., Ohta, Y., Rabinovitz, I., Stossel, T. P. & Blenis, J. (2004) *Mol. Cell. Biol.* **24,** 3025–3035.
37. Poteet-Smith, C. E., Smith, J. A., Lannigan, D. A., Freed, T. A. & Sturgill, T. W. (1999) *J. Biol. Chem.* **274,** 22135–22138.
38. Husi, H., Ward, M. A., Choudhary, J. S., Blackstock, W. P. & Grant, S. G. (2000) *Nat. Neurosci.* **3,** 661–669.
39. Morozov, A., Muzzio, I. A., Bourtchouladze, R., Van-Strien, N., Lapidus, K., Yin, D., Winder, D. G., Adams, J. P., Sweatt, J. D. & Kandel, E. R. (2003) *Neuron* **39,** 309–325.
40. Malenka, R. C. & Nicoll, R. A. (1999) *Science* **285,** 1870–1874.